EUROEM 2000 conference, UK, Edinburg 31. May - 2. June 2000
accepted for publication in: Ultra-Wideband, Short-pulse Electromagnetics 5 (Smith/Cloude, eds.)

ULTRA-WIDEBAND PRINCIPLES FOR SURFACE PENETRATING RADAR

J. Sachs*, P. Peyerl**, M. Roßberg*,
P. Rauschenbach*, J. Friedrich**

*Ilmenau Technical University, Germany
sac@e-technik.tu-ilmenau.de
**MEODAT GmbH, Germany
pey@meodat.de

INTRODUCTION

Surface Penetrating Radar (SPR) uses the properties of RF- and microwave pulses to penetrate into soil and most non-metallic building materials. Obstacles in the way of propagation cause reflections which may be received outside the body of investigation. Thus SPR can be used to detect hidden objects and to investigate the internal composition of manifold structures. The SPR antennas are moved over the surface of the body of interest touching it or retaining a certain distance depending upon the type of employment.

The difficulty of the method is in the interpretation of the gathered data as the waves are sensible to all variations of the permittivity and conductivity within the body and not only to the objects searched for. Furthermore the relative long wavelengths (cm and dm range) of the sounding waves provide radar images which are not immediately accessible to the common optical interpretations of the human being.

It is to be expected however that these drawbacks will be overcome in the future by using sophisticated software tools for data interpretation and an improved method of data gathering. Thus, SPR will be a powerful tool in many applications such as non-destructive testing in civil engineering, testing and surveillance of transport routes (roads, railways, bridges, tunnels etc.), environmental protection, detection of anti-personal landmines etc. The assumption of successful data processing is based on high quality data which could also include multistatic and polarisation information according to the specific application.

In what follows, aspects of wideband measurement technique for SPR data gathering will be emphasised. It should however be noted that high quality data in terms of SPR not only means precision measurements of scattering amplitude as a function of time (or frequency) but also of space. This - the antenna positioning - will not be regarded here. A SPR device will be considered as an LTI-system (linear time invariant). The most important technical parameters will be derived attempting to find a common base in order to compare

the different working principles. The basic wideband principles will be evaluated and a new principle will be introduced.

LTI-MODEL OF A SPR ARRANGEMENT

The aim of a SPR-device is to gather information from an object under test by the use of the scattering properties of electromagnetic waves. In order to do this, the object is touched by a wave and its reaction to this wave is measured. In the simplest case, two antennas are used (see Figure 1) - one for sending and one for receiving. The use of one antenna for both - sending and receiving - is rare because of antenna mismatch. The application of arrays with more than two antennas will however be increasingly seen as an area may be scanned in a faster way and multistatic and polarimetric data may provide more information about the body under test.

It will be usual to introduce two interfaces in a SPR arrangement. From the standpoint of an SPR-user and a simple interpretation of the images, the radiators are referred to virtual point sources (see Figure 1) which are considered as sources of spherical waves. In contrast to that, the measurement plane, to which we will restrict further consideration, is more common from the standpoint of the radar electronics. It is defined by the input/output channels ❶ and ❷ (❶, ❷, ❸, ❹, ... for antenna arrays respectively). The antennas are attributed to the measurement object by embedding the real object of interest. It is referred to [1] for relating between both interface concepts.

Regarding the measurement plane, the radar electronics represent a two-port measurement device (N-port-device in case of an array) and the body under test plus its embedding (further called system under test) may be looked upon as a linear two-port (N-port). Assuming the antenna displacement during the measurement time T_{obs} (observation time) is negligible

$$T_{obs} < \frac{c}{2\,v_{\max}\,B}, \tag{1}$$

time independent behaviour can be supposed and classical network theory can be applied. In (1), c means the propagation velocity of the wave, v_{max} the maximum displacement speed of the antennas and B is the bandwidth of the sounding wave.

At fixed antenna positions, the system under test is completely determined by its N by N scattering matrix **S**:

$$\underline{\mathbf{b}}(f) = \underline{\mathbf{S}}(f)\cdot\underline{\mathbf{a}}(f) \quad \text{for the frequency domain} \tag{2}$$

or

$$\mathbf{b}(t) = \mathbf{S}(t) * \mathbf{a}(t) \qquad \text{for the time domain} \tag{3}$$

Herein **a** is a column vector of the normalised guided waves incident to the antenna feeds, **b** is a column vector of the normalised guided waves leaving the antenna feeds and **S** is the scattering matrix of the system under test. $\underline{\mathbf{S}}(f)$ represents a set of Frequency Response Function (FRF) and $\mathbf{S}(t)$ a set of Impulse Response Functions (IRF). They are mutually referred by the Fourier Transform. Underlined symbols mean complex valued functions and $*$ refers to the convolution. The individual functions of the S-matrix will permanently change through the moving of the antennas over the ground. They represent the reflection behaviour (monostatic mode) $\underline{S}_{ii}(f, \mathbf{r}_i, \mathbf{r}_i)$ or $S_{ii}(t, \mathbf{r}_i, \mathbf{r}_i)$ of the antenna i at position $\mathbf{r}_i$ and the behaviour of the transmission path $\underline{S}_{ij}(f, \mathbf{r}_i, \mathbf{r}_j)$ or $S_{ij}(t, \mathbf{r}_i, \mathbf{r}_j)$ between the antennas i and j (bistatic mode) at positions $\mathbf{r}_i$ and $\mathbf{r}_j$. In practice, these functions form the so called radargrams (B-

scan) and radar volumes which serve to interpret the inner structure of the body under test. Generally the time representation of the measurement results are preferred because it is more accessible to human imagination. The Fourier transform however permits the change of the domains at will so that software procedures may also act upon frequency domain data if advantageous.

Regarding the current state of development, it should be stated that for simplicity only the transfer characteristic $\underline{S}_{ij}(f, \mathbf{r}_i, \mathbf{r}_j)$ or $S_{ij}(t, \mathbf{r}_i, \mathbf{r}_j)$ between one antenna pair is measured. The use of several antenna pairs at the same time is rare in practice. But a further improvement of the SPR-technology supposes antenna arrays and will only arise if sophisticated correction of systematic device errors is applied. Especially the last point demands the knowledge of the full S-matrix of the array. Only the network analyser which is not useful to employ in the field currently meets the stability requirements for error corrections with respect to random fluctuations and drift. Stable and integrated ultra wide band electronics with excellent noise suppression are required for further development of highly sophisticated SPR devices.

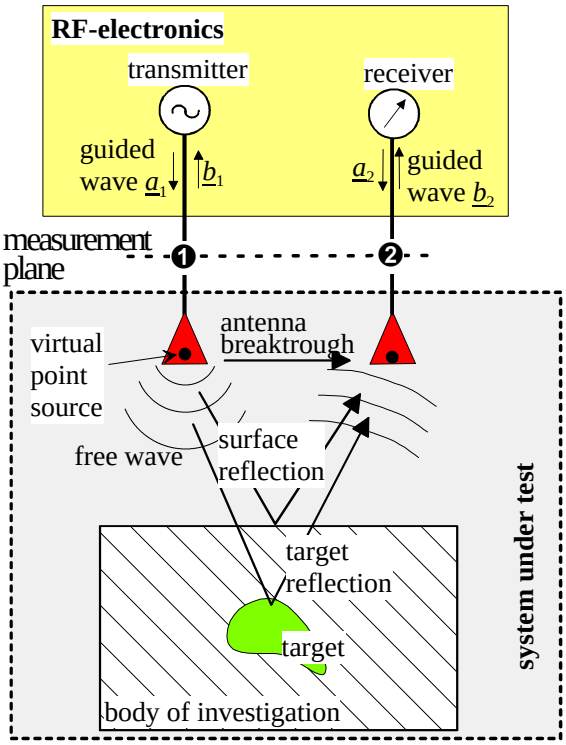

Figure 1 Basic SPR arrangement for air launching. The most important signal paths are shown. Note that in many SPR devices the wave guides between antenna and transmitter/receiver electronics degenerate to zero length.

PERFORMANCE PARAMETERS

The key features describing the performance of the radar electronics in an SPR device refer to its spatial resolution in range d_r and cross range d_{cr}, to the observation range R (unambiguity range), its sensibility for detecting weak reflecting objects and to the measurement rate r_m. These parameters have to transform to corresponding properties of the IRF or FRF measured by the radar electronics. For details on the performance of the whole radar device, the reader is referenced to [2].

To illustrate the facts, Figure 2 indicates an idealised curve of the IRF $S_{12}(t)$ of the transmission path ❶ → ❷ resulting from the simple situation in Figure 1. Pulse like sections appear which provide clues as to overall length and attenuation of the individual

propagation paths. These results are finally used to reconstruct the inner structure of the body. The first two impulses in Figure 2 will merge if the antennas are in contact with the surface.

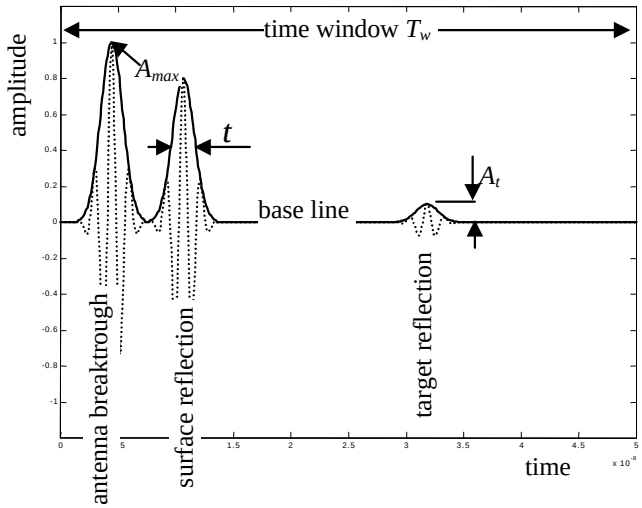

Figure 2 Idealised IRF $S_{21}(t)$ according to Figure 1

Spatial resolution. The range resolution δ_r depends upon the capability to distinguish between two adjacent pulses of equal amplitude. It is evident from Figure 2 that this may be expressed as:

$$d_r \cong \frac{1}{2} c t \cong \frac{c}{2B} \tag{4}$$

whereas t is the half-value width of the pulse envelope and B is the corresponding bandwidth. The effective usable bandwidth B of a SPR device is not only determined by the bandwidth of the stimulus signal and the antennas but also from the time jitter arising from instabilities in the transmitter and receiver circuit. The cross range resolution d_{cr} also strongly depends upon the pulse width if synthetic aperture processing is applied as well as the beamwidth $2Q$ of the antennas.

$$d_{cr} \cong \frac{ct}{2 \sin Q} \tag{5}$$

It should be noted that the carrier frequency does not apparently play any role in equations (4) and (5). It is however very critical since the stimulation band should be at frequencies as low as possible to avoid unnecessary damping of the sounding waves in the body under test. This leads finally to the requirement of a large fractional bandwidth for the electronics and the antennas which is not always easy to achieve in practice.

Observation range: The observation range R (unambiguous range) depends upon the length of the time window T_w for which the impulse response is measured. In the case of periodical stimulation signals, it is limited to its period T to avoid time aliasing.

$$R = \frac{1}{2} c T_w \leq \frac{1}{2} c T \tag{6}$$

Measurement rate: The time which is needed to gather all the data which is included in a complete IRF or FRF will be called observation time T_{obs}. As such, the repetition rate r_m for the measurement is

$$r_m \leq T_{obs}^{-1}. \tag{7}$$

In case of an antenna array of L elements the measurements rate r_m may be reduced by the factor L [3][4].

Detection limit: The detection limit describes the capability to find still small scattering amplitudes in the IRF that are caused either from small scatterers with poor dielectric contrast or by propagation loss. The sensitivity of an SPR device is limited by all deviations from a straight flat base line within the IRF if not any scatterers are present. This means, referring to Figure 2, that only the first impulse may appear. All deviations from that represent errors which limit the sensitivity.

Depending upon the error phenomenon, several parameters are usual to characterise these deviations by the notation signal-to-perturbation-ratio. Let us suppose that the maximum detectable amplitude of the IRF is A_{max}, then the following three values can be defined:

signal to noise ratio L_n: $$L_n\left[\mathrm{dB}\right] = 20\log_{10}\frac{A_{\max}}{x_{eff}} \tag{8}$$

peak to side lobe ratio L_{sl}: $$L_{sl}\left[\mathrm{dB}\right] = 20\log_{10}\frac{A_{\max}}{x_{sl}} \tag{9}$$

peak to spurious ratio L_s: $$L_s\left[\mathrm{dB}\right] = 20\log_{10}\frac{A_{\max}}{x_s} \tag{10}$$

x_{eff} is the effective value of random noise , x_{sl} the maximum side lobe amplitude and x_s the maximum spurious lobe amplitude. Note that the values above are in respect to an IRF which may also result from signal processing, thus A_{max} can be much higher than the real measured signal amplitudes. Corresponding holds for the perturbation values x_{eff}, x_{sl} and x_s which may be reduced in the digital domain by averaging, deconvolution and certain kinds of error correction.

It is distinguished between L_{sl} and L_s for the following reason: L_{sl} is caused by linear effects (ripples in the stimulation band, abrupt cutting of frequency band, device internal reflections etc.) and L_s is the result of non-linear effects in the receiver and crosstalk by clock lines or similar. Very hard constraints with respect to L_{sl} may arise for shallow target detection since the scattering peak is located very close to the main lobe where the strongest side lobes can also be found. Note however that the antenna is often the most critical component in this respect.

Finally, the maximum depth / minimum size of a scatterer may be estimated from the effective system performance L_{sp} [1]:

$$L \quad L_{\min} + \min\{ \quad L \ , L \ \} \tag{11}$$

[1] Note, that system performance is seen as a ratio between max. transmitter amplitude and effective noise amplitude, whereas L_{sp} refers to a more usable value respecting receiver overload, non-linearity etc.

L_{min} corresponds to the attenuation of the strongest transmission path, e.g. antenna breakthrough or surface reflection.

The key to a high side lobe and spurious suppression is sophisticated hardware design. These phenomena are however systematic errors, thus they may be corrected by an appropriate calibration routine. With regards to linear effects, the corresponding methods are well known from network analyser theory (response-, 3-term-, 12-term-calibration etc.). Comparable procedures seems also to be applicable to reduce the influence of spuriousness. It must however be noted that software corrections are only successful if all the required data[2] is available and the system is working stable over time – that is equidistant sampling and poor in random noise, jitter and drift.

MEASUREMENT PRINCIPLES

Three basic measurement principle are known which are mainly distinguished by the kind of stimulus signal that is applied. In what follows, they will be shortly introduced for the example of a transfer measurement and their advantages and disadvantages will be mentioned.

Impulse technique: The impulse technique uses the fact that the convolution (3) may be simplified if the stimulus represents a Dirac-like pulse $d(t)$. Referring to the notations in Figure 1 this provides

$$b_2(t) \sim S_{21}(t) \quad \text{for} \quad a_1(t) \cong d(t). \tag{12}$$[3]

Since $b_2(t)$ can be measured by an oscilloscope, the image of its screen represents the IRF if the bandwidth of the stimulus pulse is larger than the bandwidth of the antennas. Nearly all commercial available SPR-devices work on this principle because of its simple technical implementation. In order to concentrate the energy of the stimulus in the pass band of the antennas, monocycles are rather used than pulses. The impulse generation is largely based on avalanche transistors or step recovery diodes and sequential sampling circuit serves as receiver front-end. In the following, some problems of pulse systems are summarised.

Often, the measurement rate is relatively low because the avalanche transistors need time to recover from the pulse shocks and moreover only one data sample is captured per pulse. This limits the use of the method in large arrays and high-speed applications. It is reported in [6] on a module with improved measurement rates to overcome this drawback. Peak power is however lost.

The mean energy of a pulse is very low even for relative high amplitudes and the noise bandwidth of the sampling gates is very large. The method is therefore sensitive to random noise. The noise influence may be suppressed either by averaging (further reducing the measurement rate) or by generating extreme high voltage impulses having a peak power up to 100 MW and more [7]. This however represents no practical solution for an industrial application of the SPR method.

The sampling gate control is undertaken by voltage ramps. Thus, any inadequateness of these ramps such as non-linearity, temperature drift or noise translates to errors of the

---

[2] For correction of linear errors this means for example, that the full S-matrix must be known which drastically increases the system complexity.

[3] The vectors $\mathbf{r}_i$ and $\mathbf{r}_j$ of antenna location and the matrix representation for multi-channel systems will be omitted for simplicity in the following

time axis (drift, jitter and non-equidistant sampling). However, the ability of the sampling control to blank-out the troubling antenna breakthrough and surface reflex is often of advantage in pulse methods for deep sounding. On the other hand error corrections as mentioned above are less promising in cause of the drift susceptibility of sequential sampling. Possibly new system designs may overcome these drawbacks [5].

Sine Wave Technique: The sine wave technique determines the IRF $S_{21}(t)$ by the roundabout way over the complex FRF $\underline{S}_{21}(f)$:

$$S_{21}(t) = \mathrm{IFT}\{\underline{S}_{21}(f)\} \sim \mathrm{IFT}\{\underline{Y}_{ba}(f)\} \text{ for } Y_{aa}(f) \cong C \tag{13}$$

Herein are IFT{} the inverse Fourier transform, $\underline{Y}_{ba}$ the complex valued cross spectrum between stimulus and receiving signal and Y_{aa} is the real valued auto spectrum of the stimulus which should be constant over the bandwidth of the antennas.

In the technical implementation, a sine wave is stepped or continuously sweeped over the band of interest and the cross spectra is measured via quadrature modulators in the IF-band of an heterodyne receiver (network analyser, vector receiver). The step width of the frequency steps determines the unambiguous range. Sometimes, for deep sounding purposes, gated network analysers are used in order to blank out leakage signals such as ground reflection or antenna coupling [8]. Attention should be paid to the inverse Fourier transformation if the stimulation band is smaller than the antenna bandwidth. The side lobes in the impulse response are no longer determined by the antenna response but rather from the abrupt breakdown of the stimulation spectrum Y_{aa}. These side lobes may be suppressed by windowing the data before transformation but this results in slightly reducing the range resolution. The potential of the method is its excellent drift stability and random noise suppression because of the narrow band receivers as well as its flexibility within the choice of the stimulation band. It is however also the most expensive and slowest method.

The FMCW-radar represents an attractive alternative to the stepped frequency radar because of its simplicity, measurement speed and dynamic range. It is based on a homodyne receiver using a stimulus continuously sweeped over an appropriate band. Particular problems arise by a non-linear VCO characteristic thus further expense is necessary (PLL, reference delay or similar). A FMCW-radar is only able to determine the real part of the FRF $\mathrm{Re}\{\underline{S}_{21}(f)\}$ due to the lack of a quadrature modulator. Consequently, sophisticated calibration routines such as for network analysers are not available and the IRF can only incompletely calculated. A network analyser is more robust against spuriousness caused by a non-linearity in the mixers than the FMCW-principle since its narrow IF-filters may partly reject intermodulation products.

Correlation Technique: From the theoretical standpoint, the correlation technique is the most flexible method of system identification since it is not fixed to a certain kind of test signal. Comparable to equation (12) the IRF of a device may also be determined by:

$$y_{ba}(t) \sim S_{21}(t) \quad \text{for} \quad y_{aa}(t) \cong d(t) \tag{14}$$

in which the correlation functions y_{ba} and y_{aa} are defined according to ($x = a_1$ or b_2):

$$y_{xa}(t) = \int_{-\infty}^{\infty} a_1(t) \cdot x(t+t)\,\mathrm{d}t\,. \tag{15}$$

The side condition in equation (14) is much more weaker than that in equation (12), because it does not demand a specific shape of the test signal. It refers only to a flat spectrum: FT$\{y_{aa}(t)\}$ → constant. In practice this means that the auto correlation y_{aa} should be short compared to the impulse response and with few side lobes. The opportunity to choose different types of test signals opens the possibility to optimise the measurement method with respect to several aspects. The favourable noise suppression of the correlation is based for example on this feature because high energy signals with low amplitudes (small crest factor) can be applied. The handling of such signals is also often easier than that with high peak power. The problem is however to find an appropriate procedure for solving the correlation integral (15).

Several solutions are known from which the matched filtering is the most common but these filters cannot be built for ultra wideband purposes with low centre frequencies. Thus matched filtering by analogue filters is not applicable for SPR purposes.

White random noise is a good choice for a stimulus signal if interactions between different radar devices should be prevented or if the device is working in a non-cooperative environment (military application). In that case, the conversion of (15) is based on a mixer, a stepped or sweeped delay line and a low-pass filter [9], [10]. The bottleneck is however the delay line which is expensive to manufacture and its properties limit the overall device behaviour to a large extent. This makes it unattractive for industrial SPR use.

The answer for ultra wideband principles can only be to carry out the correlation/matched filtering in the digital domain. The simplest way to do this is the so-called polarity correlator. It captures only the zero crossings of the signals. Multiplication, delay and summation is undertaken by digital circuits (XOR, shift register, counter for bit-wise summing). The method could not be realised up till now despite its simplicity. One reason may certainly be found in its time consuming data capturing.

A new ultra wideband principle working on a digital correlation/matched filtering will be shortly introduced in the following (see also [3], [4] for more information).

MBC-RADAR

As noted above, the correlation technique opens the possibility to freely choose the test signal. Thus a great deal of other constraints may be taken into account in finding an optimum solution:

- Wideband signal (general requirement),
- Low crest factor signal in order to generate and handle high (mean) power signals (high signal to noise ratio L_n!) by simple electronics,
- Periodic signal in order to apply undersampling for signal acquisition and averaging for noise suppression,
- Simple and stable generation in the RF- and microwave range,
- Simple and stable generation of acquisition clock,
- Simple and fast correlation algorithm (digital matched filtering),
- Ability to simply synchronise and to control multi-channel arrangements,
- High measurement rate,
- Integration friendly electronics, and
- High flexibility with respect to the technical implementation.

The **M**aximum length **B**inary sequence **C**orrelation Radar (MBC-Radar) meets these requirements. The maximum length binary sequence (MLBS) is a special kind of binary random code. Its time shape, auto correlation function and spectrum is indicated in Figure 3.

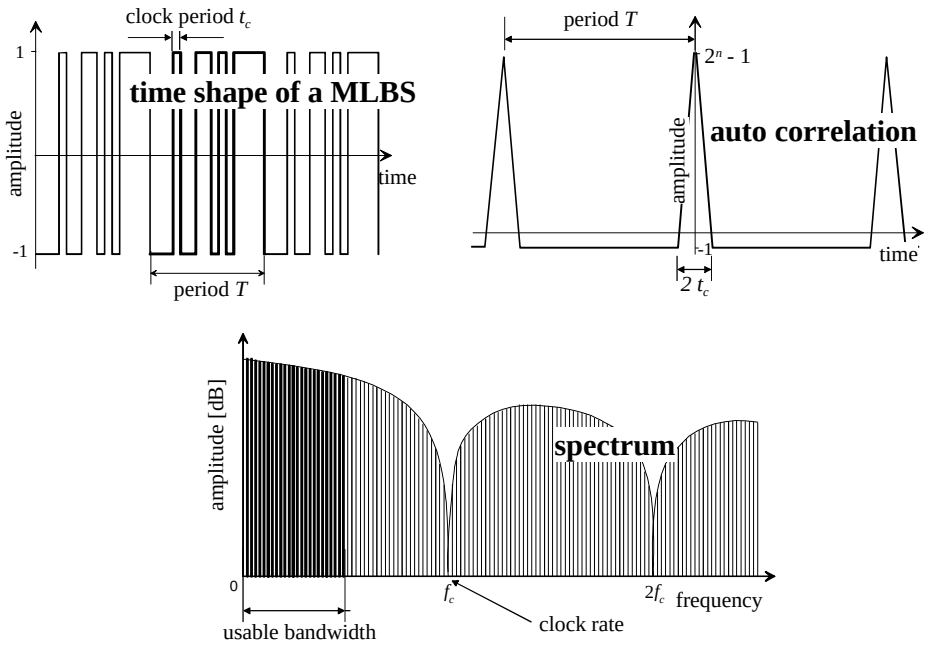

Figure 3 Time shape, auto correlation function and spectrum of a MLBS. For a better graphical representation the shown spectrum applies to a MLBS of higher order than used in the other diagrams.

An MLBS of order n may be generated by an n-stage shift register using an appropriate feedback. The MLBS period is $T = (2^n - 1)t_c$, where t_c is the period of the system clock. Regarding the spectrum in Figure 3, it is useful to fix the equivalent sampling frequency of the receiver circuit to the clock frequency $f_c = 1/t_c$ that means one sample per elementary pulse of the sequence. Thus the usable bandwidth B is limited to the range $0 \le f < f_c/2$ of the MLBS-spectrum. As long as the maximum clock rate of the shift register is respected, there are no limits in the choice of this rate. As such, the measurement system may be simply adapted to a specific measurement situation by varying the clock rate. Table 1 compares different circuit technologies with respect to the maximum bandwidth within reach.

	max. clock rate	max. bandwidth	
commercial CMOS-IC	200 MHz	100 MHz	experimental verified
commercial ECLinPs-IC	1 GHz	500 MHz	
0,8 µ Si/SiGe-IC HBT (customer IC)	up to 12 GHz	6 GHz	
0,25 µ SiGe:C HBT BiCMOS	20 GHz	10 GHz	estimated
0,18 µ CMOS	20 GHz	10 GHz	
GaAs	40 GHz	20 GHz	

Table 1: Shift register circuit technology versus bandwidth

One of the most important features of the new method is, that the sampling frequency f_s in the receiver may be derived in stable manner from the clock rate f_c by an m-stage binary clock divider so that $f_s = 2^{-m} f_c$. Since the period length T of an MLBS always differs by one clock period from a power of two 2^m periods of the MLBS are needed to acquire the complete data set with the equivalent sampling frequency f_c.

The practical implementation of the principle is demonstrated in the block diagram of Figure 4. Except for the emphasised part, all components are low cost commercial ICs. The

whole system is triggered by a stable clock generator that pushes an n-stage shift register and an m-stage binary divider. The shift register generates the MLBS stimulus $m(t)$ and the divider delivers the sampling clock f_s, which drives the S&H circuit, the ADC and an averager. Finally, a digital signal processor (DSP) calculates the cross correlation $y_{bm}(t)$ which is approximately equal to the IRF of the system under test:

$$y_{bm}(t) \sim S_{21}(t) \text{ if } \begin{cases} y_{aa} = y_{mm} \cong d(t) \\ \text{and} \\ S_{21}(t \geq T) < e \end{cases} \tag{16}$$

Due to the periodicity of the MLBS, the function y_{bm} represents a cyclic cross correlation function which can be calculated very fast by the Hadamard-Transform.

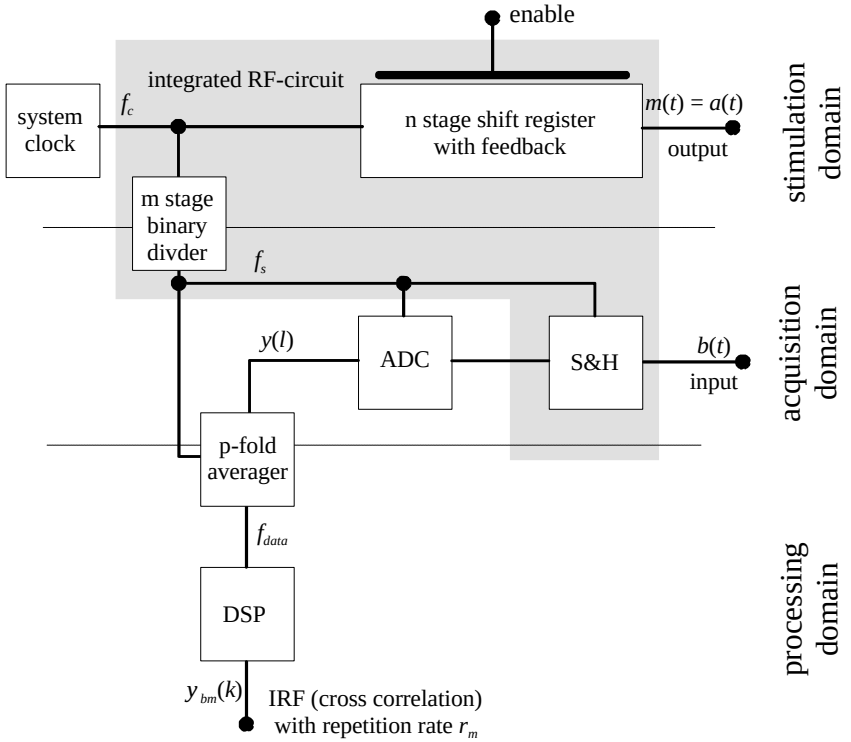

Figure 4 Block diagram of the UWB front end. The emphasised section should be integrated to achieve a bandwidth greater than 500 MHz.

The p-fold averager matches the signal acquisition rate f_s to the processing speed of the DSP by reducing the data rate to f_s/p. Simultaneously, it increases the dynamic range of the captured signal. The dynamic range L_n with respect to random noise and the overall observation (correlation) time T_{obs} results in:

$$L_n[dB] \cong 6b + 3n + 10\lg_{10} p \tag{17}$$

$$T_{obs} = r_m^{-1} \cong 2^{n+m}\, p\, t_c \tag{18}$$

Here b is the number of effective bits (ENOB) of the acquisition circuitry (S&H and ADC). The last two terms in (17) represent the signal processing gain by which the dynamic of the real signals is improved. L_{sl} is infinity for an ideal MLBS, independent from its order and L_s is mainly determined by the linearity of the receiver circuit (ADC, S&H). The maxi-

mum measurement rate of the method is mostly fixed by the DSP-hardware. The determination of 16 000 IRFs (consisting of 511 points) per second and more seems to be possible with modern signal processors.

The structure of the MBC-radar is divided into three domains each having its own processing speed (see Figure 4). The interconnection between the different sections is formed by programmable digital blocks (divider, averager). This provides a great flexibility to adapt the system parameters to the requirements of the actual measurement and it permits a high flexibility within system design and manufacture. It should be further noted that the simple clock scheme and the ability to enable/disable the MLBS shift register simplifies the creation of multi-channel arrangements like antenna arrays since multiplexing of RF-lines is no longer needed.

CONCLUSION

SPRs will achieve wide industrial employment if they succeed in offering adapted solutions for a specific class of tasks. These solutions will be based on sophisticated methods of digital data processing which require stable, high quality data, increasingly gathered by antenna arrays. The future challenge on RF-electronics is to meet these requirements.

The main demands on the RF-electronics of a SPR device results from a large fractional bandwidth and a high dynamic range. Several wideband methods were presented. Impulse principles are the most frequently used followed by the FMCW-radar. Sine wave techniques are very flexible. They are particularly suited to laboratory experiments but their low measurement speed may limit field use. A new ultra wide band principle was introduced which is based on a maximum length binary sequence. It is a promising method to capture high quality data and it is suited for application in antenna arrays.

REFERENCES

[1] R. Zetik, J. Sachs, B. Schneegast: Evaluation of antenna pattern for radiation in solid media. Proc. of IRS 98, vol. II, p. 629-38

[2] T. Scullion, C. L. Lau, T. Saarenketo: Performance Specification of Ground Penetrating Radar. Proc. of GPR'96, p. 341-6

[3] J. Sachs, P. Peyerl, M. Rossberg: A New UWB-Principle for Sensor-Array Application. Proc. of IMTC/99, vol. 3, p. 1390-5

[4] J. Sachs, P. Peyerl: Ein neues Breitbandmeßverfahren für das Basisband. Workshop of German IEEE/AP Chapter on Short Range Radars, Technical University Ilmenau, July 1999 (http://www.meodat.de/veroeff.htm)

[5] A. Schukin, I Koploun, A., Yarovoy, L. Ligthart: Evolution of GPR Antennas, Pulse Generators and Sample Recorders. Proc. of AP2000, Davos, Switzerland

[6] J. Warhus, J. Mast, S. Nelson: Imaging Radar for Bridge Deck Inspection. http://wwwlasers.llnl.gov/lasers/idp/mir/files/warhus_spie/spiepaper.html and other publications around the MIR-module.

[7] P.R. Bellamy: Ultra Wideband Radar: Current and Future Techniques. Proc. of EUROEM 1995, p. 1620-6

[8] G. F. Stickley, D. A. Noon, M. Cherniakov, I. D. Longstaff: Current Development Status of a Gated Stepped-Frequency GPR. Proc. of GPR'96, p. 311-5

[9] R. M. Narayanan, Y. Xu, P. D. Hoffmeyer, J. O. Curtis: Design and performance of a polarimetric random noise radar for detection of shallow buried targets. Proc. of SPIE, vol. 2496, p. 20-30, Orlando 1995

[10] R. Stephan, H. Loele: Ansätze zur technischen Realisierung einer Geschwindigkeitsmessung mit einem Breitband-Rausch-Radar. Workshop of German IEEE/AP Chapter on Short Range Radars, Technical University Ilmenau, July 1999